

GeoArch

Report 2006/09

Archaeometallurgical residues from
Coldfurrow, Lyonshall, Herefordshire

Dr Tim Young
25th June 2006

Archaeometallurgical residues from Coldfurrow, Lyonshall, Herefordshire

Dr T.P. Young

Abstract

The assemblage from Coldfurrow comprises approximately 11kg of material, dominantly slag but also including hearth lining, derived from iron smithing. The material was recovered from a very restricted area of the site, close to a pit with burnt sides, yielding both macro- and micro-residues from smithing, which may have been an unusual form of smithing hearth. The slag assemblage is dominated by smithing hearth cakes (SHCs) of which 14 complete examples provide 7.8kg of the total and small fragments much of the remainder.

The SHCs are unusual for Romano-British smithing assemblages on two grounds. Firstly they possess an extremely iron-rich composition, which may indicate the use of a tuyère, or some other unusual feature of hearth construction, that has led to a diminished supply of silicate material from the hearth wall to the slag generating process. Secondly the relatively large size and weight of the individual SHCs distinguishes the material from most described Romano-British smithing assemblages, but parallels can be found from other sites where bloomsmithing is believed to have been undertaken.

The iron-rich slags have a granular texture due to a heterogeneous distribution of wustite, produced during early stages of cooling. The high-iron nature of the slags has also led to the olivine mainly being very close to end-member fayalite. The incorporation of fuel ash into the slags is very localised, with development of leucite-wustite syntectics, in many places associated with, or intergrown with, calcic olivines, particularly around vesicles. Exploration of the mass balance for slag production hints at the use of quartz flux during production of most of the slag cakes. One particularly large SHC (2.1kg) has a basal zone that was especially iron rich, reaching over 80 vol% wustite, and has a rather different trace element composition, particularly a relative depletion of the light rare earth elements. These differences may imply that this material might have been produced during a slightly different process from the bulk of the material, possibly during the early stages of bloomsmithing.

Contents

Abstract	1
Methods	1
Results	
General	2
Detailed analysis	
Sample descriptions	3
SHC chemical composition	3
SHC microstructure & microanalysis	3
Overview	3
Details	4
Modelling of chemical composition ..	4
Interpretation	5
Discussion	5
References	6
Plate Captions	7
Catalogue	8
Figure 1: Upper crust-normalised REE profiles ..	9
Figure 2: Lining-normalised REE profiles	9
Table 1: List of smithing hearth cakes	3
Table 2: Comparison of SHC weight statistics	3
Table 3: Summary of mass balance modelling	4
Table 4: Major elements by XRF	10
Table 5: Minor and trace elements by ICP-MS	10
Table 6: Calculated ratios and iron content	11
Table 7: Mass balance calculations	12

Methods

All materials were examined visually with a low powered binocular microscope as part of the evaluation (Young 2004). The evaluation identified the assemblage as having been produced during iron working (smithing) and noted that many of the smithing hearth cakes (SHCs) from the site have a somewhat unusual granular texture and that there was a wide range of SHC weights. A follow-up programme of analysis was designed to investigate the cakes in more detail. General description of the assemblage in this report is based on, and updated from, that in the evaluation report

Six SHCs were selected as being representative of the material. Each of the six cakes was first cleaned thoroughly, and then cut longitudinally, with a slice taken on one side of the centreline being further subdivided to provide specimens for chemical analysis and microscopy. One of the six cakes (LYCF04-5) was sufficiently thick to require two sets of samples, one from the basal part and one from the upper. The evaluation proposed detailed electron microscopy of four samples; after cutting the SHCs, two were determined to have a high degree of alteration (LYCF04-1 and LYCF04-6) and preparation of polished block from these two was not pursued, leaving 5

samples from 4 SHCs. Chemical analysis was undertaken of all 7 SHC specimens, plus 2 samples of hearth lining (LYCF04-7 from c1573; -8 from c1511).

Microscopy was undertaken on the LEO S360 analytical electron microscope in the School of Earth, Ocean and Planetary Sciences, Cardiff University. Microanalysis was undertaken using the system's Oxford Instruments INCA ENERGY energy-dispersive x-ray analysis system (EDX). All petrographic images presented in this report are backscattered electron photomicrographs.

Chemical analysis was undertaken using two techniques. The major elements (Si, Al, Fe, Mn, Mg, Ca, Na, K, Ti, P) were determined by X-Ray Fluorescence using fused beads, on the Open University Earth Science Department's Wavelength-Dispersive X-Ray Fluorescence (WD-XRF) system. Whole-specimen chemical analysis for minor and trace elements was undertaken using samples in solution on the ThermoElemental X-series Inductively-Coupled Plasma Mass Spectrometer (ICP-MS) in the School of Earth, Ocean and Planetary Sciences, Cardiff University.

Context	weight	sample	proportion	original weight
1511	176		100%	176
1511	180		100%	180
1573	210	1	100%	210
1561	260	6	100%	260
1526	266		100%	266
1561	290		100%	290
1526	390		100%	390
1531	394		100%	394
1511	450	2	100%	450
1103	564		100%	564
1523	750	4	100%	750
1526	765	3	100%	765
1523	1128		90%	1015
1531	2077	5	100%	2077

Table 1: list of complete, probably complete and reconstructable SHCs, sorted by estimated original weight (in gram).

Results

General

The assemblage totalled approximately 11kg of residues, dominantly smithing hearth cakes (SHCs) and fragments of hearth lining. Complete (or almost complete) SHCs comprised 7.8kg of the assemblage (14 pieces). A catalogue of the assemblage is presented below (p. 8). The SHCs ranged from 176 to 2077g in weight, with an average weight of 564g (Tables 1 and 2).

During evaluation of the assemblage (Young 2004) three groups of residues were identified, all originating during iron-working (smithing). The inner enclosure ditch and the square ditch within the enclosure (c1103, c1511, c1523, c1526) apparently yielded medium sized, plano-convex SHCs with a prominent granular texture, the "smithing pit" (c1561) was identified as yielding mainly examples of small, flat, slab-like, SHCs, also with a granular fabric and thirdly

the terminal of the square ditch (c1531) produced an example of a large plano-convex SHC. During full examination of the material the continued separation of these groups was determined not be justified, with the recognition of some additional small SHCs in the enclosure ditches providing a stronger link between the assemblages.

In general the SHCs show a vesicular texture with a granular structure. The main suite of SHCs ranged up to about 160mm length, 120mm width and 55mm thick, with a weight of up to approximately 1kg. Some of the smaller cakes were of a thin tabular shape, rather than a plano-convex form. All the cakes were typically rusted and dense, some showing signs of cracking due to the expansion of contained metallic iron pieces on rusting. The exceptionally large SHC from c1531 was broken, had a total weight of 2.1kg, and had a plano-convex shape measuring 190mm long by 150mm wide and a maximum of 70mm deep.

	Coldfurrow	Carrigoran	Coolamurry	Carmarthen	Marsh Leys	Cowbridge
count	14	18	41	136	30	
min	176	124	100	100	56	175
max	2077	3866	2586	820	824	700
mean	564	553	388	227	333	403
<500	64%	72%	83%	94%	77%	
<1000	86%	89%	95%	100%	100%	100%
>1000	14%	11%	5%	0%	0%	0%
>3000	0%	6%	0%	0%	0%	0%
modal 100g class	200-300	100-200	100-200	100-200	100-200	

Table 2. Comparative statistics for SHC weights for Coldfurrow with two early medieval Irish sites employing tuyères and probably undertaking some bloomsmithing (Carrigoran, Co. Clare, Young 2006b; Coolamurry, Co. Wexford, Young 2006a) and three Romano-British sites probably only undertaking blacksmithing (Carmarthen, Crew 2003; Marsh Leys Farm, Beds., Young 2005; Cowbridge, Barford 1996).

Pieces of fired hearth lining were recovered from five contexts, with much of the material showing a well-vitrified face. One interesting feature was that several pieces showed a convex vitrified face. This may indicate the material was derived from the margins of the zone above the tuyère/blowhole where melting often results in a hollow being produced in the wall. The material from the "smithy" pit and the SW side of the square ditch was slightly different to the material from the N side of the square ditch and the main enclosure ditch, being in a slightly finer grained material compared with the micaceous lining, which fired to a pink colour, which was found in the northern areas. Whether this small sample is sufficient to suggest derivation from two different hearths is uncertain.

The slag pieces from the smithing pit had concreted material attached to the outside of the specimens that was rich in charcoal fragments and flake hammerscale. Gridded magnetically collected samples from the area of this feature yield small quantities of flake hammerscale, along with magnetic fired clay, stone and slag particles. The volume of collected material is small, but is greatest in samples:

E=41.4 N=107.0/107.2/107.4

E=41.6 N=107.0/107.2

E=41.8 N=107.0/107.2/107.4

Detailed analysis

Sample descriptions

Detailed investigation of a suite of SHCs was undertaken. Two examples (LYCF04-1 and -6) of the small SHCs present in the pit feature (c1561) were examined (unfortunately both proved too weathered for detailed microscopy), three examples (LYCF04-2, -3, -4) were selected from the medium-sized SHCs from the ditches and the large SHC from the ditch terminal (LYCF04-5) was also investigated:

LYCF04-1. c1573. 210g. 80x70x30mm. A very irregular smithing hearth cake. The base is very rusty. Vesicularity decreases upwards. The cake is rather weathered. Sample for polished block includes the top, but was determined to be too weathered for microscopic analysis.

LYCF04-2. c1511. 450g. 120x100x40mm. Base is rough to microprilly. Top has raised slag lobes. Charcoal rich throughout, with finer material towards base. Samples taken through whole thickness.

LYCF04-3. c1526. 765g. 160x90x60mm. Smithing hearth cake has a vesicular bowl, filled by rusty charcoal rich material, above this is a denser central raised area. The polished block extends through the denser zone from the top towards the rusty zone. The analytical samples are elongate passing through the cake.

LYCF04-4. c1523. 750g. 110x100x50. Base prilly, top blown smooth proximally. Sediment inclusions occur low on proximal end (in polished block). Appears to be a double layer cake externally, but this is not obvious in the internal texture. This SHC is significantly denser than the other samples.

LYCF04-5. c1531. 1960g. 210x160x80. Internally homogeneous, vesicular and charcoal rich. The base is obscured, the top is dimpled.

LYCF04-6. c1561. 260g. 100x80x40. Rusty base, open grey porous main slag, browner and denser at top. Samples go all way through. This cake was determined to be too weathered to justify detailed microscopy

SHC chemical composition

The key feature of the chemical composition of the slags is their very high iron content (range 56-64 elemental wt%; range 73-82 wt% when calculated as FeO; 81-91 wt% when quoted as Fe₂O₃). Silica contents range from 8.1 to 15.4wt% and alumina 1.5 to 2.7wt%. All the slags were thus considerably more iron-rich than fayalite. Such iron-rich silica-poor compositions are unusual, and indicate a rather low degree of fluxing of iron lost from the workpiece. Concentrations of other major elements (Mn, Mg, Ca, Na, K) are also all very low.

Trace element contents of the slags are all generally low.

Comparison of the rare earth element (REE) composition of the slags and lining samples apparently shows a simple, almost dilutional, relationship for most samples, with very little fractionation. REE profiles for the slags are presented both as Upper Crust-normalised values (after Taylor & McLennan 1984; Fig 1), but also normalised against the lining LYCF04-7 (Fig. 2). In this lining-normalised diagram, the slags fairly flat profiles for almost all samples, compatible with a wholesale incorporation of lining material without significant fractionation for all samples, except LYCF04-5a, which shows a strong relative depletion in the light REE (LREE). Normalisation of the slags against lining LYCF04-8 produced profiles with slight inclination downwards towards the LREE, so are interpreted as being a less useful normalisation.

The lining samples have fairly typical, although somewhat differing, analyses; LYCF04-7 is rather siliceous and has a rather low REE content, whereas LYCF04-8 has a high REE content. LYCF04-8 shows a fairly flat REE profile when normalised against upper crust (fig 1), with values average approximately 1.9 times upper crust. LYCF04-7 has a profile inclined to the LREE, indicating higher enrichment of the HREE with respect to upper crust, with an average of approximately 1.3 times upper crust concentrations.

SHC microstructure and microanalysis

Overview

All the samples show some degree of alteration, with both oxides and silicate minerals affected. Open vesicles and clasts of surviving fuel material are often the focus of the greatest alteration. The following descriptions, however, focus on the evidence for the primary mineralogy rather than the alteration.

The SHCs show some consistent features, despite the differences between them. Because the internal structure of the SHCs is so heterogeneous, establishing typical, or overall, mineralogical compositions is not possible. All the cakes show a substantial development of early wustite, which is at a maximum in the lower part of LYCF04-5, with wustite comprising well over 80 vol%. The upper part of LYCF04-5 has wustite comprising approximately 50%, with 37% olivine. The three medium-sized cakes have

variable wustite concentrations in the range of 30-45 vol%.

The heterogeneous distribution of wustite is apparently controlled in most of the material by the distribution of vesicles within the slag during wustite growth. It would appear that this pattern of wustite formation is the controlling factor for the granular texture noted in hand specimen. The early formed wustite grew with a highly vesicular slag, with some of the vesicles surviving through to eventual cooling of the slag, but most became filled with a more fluid fayalite slag.

Olivine comprises only a small proportion of the lower part of LYCF04-5, and 28-43% of its upper part, but is present in slightly higher concentrations in LYCF04-2, 3 and 4. The olivine is, in general, very close to end-member fayalite, with low magnesium levels restricting the forsterite component of the cores of the olivine crystals to levels below 6%. Calcium enrichment is marked in olivines associated with areas bearing leucite, with up to 30% Ca substitution recorded, although values of up to 10% are more common.

Leucite is abundant, particularly around the sites of former vesicles, where it may form vesicle rims (either alone or in a syntectite with wustite) and may also occur as intergrowths of leucite-wustite with a Ca-rich olivine. Smaller quantities of leucite-wustite may occur as an interstitial phase away from surviving evidence for former vesicles. These features strongly suggest that both K and Ca have been concentrated in these regions by absorption from the fuel ash.

Details

LYCF04-2: The body of this specimen had a microstructure with prominent early wustite (43%), overlain by elongate olivines (48%), with interstitial glass bearing fine olivine dendrites (total 9%). Towards the top of the specimen the texture becomes more heterogeneous, with large vesicles infilled with a n olivine-dominated material, with elongate olivine up to at least 800µm in length (varying from Fa96 on the margin to slightly more magnesian Fa93 in the core), radiating from origins on the vesicle wall, and bearing only a small proportion of fine wustite together with an interstitial glass. These infilled vesicles may have complex rims of leucite, or of a leucite-wustite syntectic.

The raised lobes of slag on the upper surface have an olivine-dominated microstructure (olivine rather equant and up to 500µm diameter, with a relatively Mg-rich core composition of $(\text{Fe}_{1.82} \text{Mg}_{0.16} \text{Mn}_{0.01} \text{Ca}_{0.02})\text{SiO}_4$, with either an interstitial glass bearing olivine dendrites $(\text{Fe}_{1.92} \text{Mg}_{0.02} \text{Mn}_{0.01} \text{Ca}_{0.05})\text{SiO}_4$ and very occasional small grains of hercynite, or with an interstitial leucite-wustite syntectic. Wustite comprises less than 5% of this material overall.

LYCF04-3: The lower part of this specimen is characterised by coarse (blebs of at least 50µm) early wustite, followed by a rather block olivine (with slightly magnesian Fa93Fo6 cores) which fills many of the former vesicles within the wustite texture. Other vesicles remained open and are mainly filled with hydrated iron oxide weathering products. Textures seen near the top are rather similar, although the details are locally obscured by alteration. Some vesicles in the centre of the sample show partial filling by olivine that has an olivine-wustite syntectic at its core. Other examples show a strong vesicle rim of a leucite-wustite syntectic, which in some places

appears to have intergrowths with olivine. This olivine is slightly calcic reaching about 5% Ca substitution.

In general wustite comprises from 30 to 45% of the local texture of the specimen.

LYCF04-4: this specimen shows the base of the SHC, which has a microstructure of elongate olivine up to 2mm in length radiating from points on the basal surface. The basal 500mm contains no wustite, but fine dendrites precede the radial olivine for most of the 2mm basal zone. The lowest 4mm of the cake averages 25% wustite, with most of the remainder being olivine. Above this the texture becomes more heterogeneous, with coarser wustite patches between what appear to be infilled vesicles bearing more olivine-rich fills. This heterogeneous material averages approximately 32% wustite, 59% olivine and 9% of interstitial materials including glass, leucite-wustite syntectic (some intergrown with an fayalite with 6-10% Ca substitution) and fine dendrites of Ca-rich olivine (possibly up to 30% Ca substitution)

LYCF04-5: The lower part of this cake is seen in LYCF04-5a. The material is dominated by wustite, which exceeds 80% in most areas. The wustite forms tightly packed irregular shapes, with diameters of up to 200µm. Within the wustite-dominated material, former vesicles are filled with elongate olivines, with an interstitial leucite-wustite syntectic and a glass (usually highly altered) bearing what appear to be tiny (2-5µm diameter; too small for EDS microanalysis) tubular olivine crystals.

A section of the upper part of the cake is seen in LYCF04-5b. This part of the cake is more heterogeneous, and more strongly resembles the other specimens from the site. The base of the section shows a very abrupt contact between a material dominated by olivine with the coarse wustite of the lower part. These silicate-rich slags contain abundant leucite-wustite syntectic grains near the contact with the coarse wustite, and in places these seem intergrown with the olivine, which reaches about 5% Ca substitution. Higher in the cake there is less leucite-wustite and more of an interstitial glass bearing fine late olivine dendrites. The upper part of the cake still contains a primary wustite phase, but this is less dense and the blebs smaller than in the lower part. Samples above, but close to the interface with the wustite rich material show around 42% wustite, 49% olivine and 9% interstitial phases, with increasingly higher samples showing 57, 39, 62% wustite, 30, 43 and 28% olivine, with the interstitial material varying from 9 to 16%. These figures show considerable heterogeneity, which is probably largely associated with a rather patchy growth of the early wustite, although there are rather fewer clear examples of infilled vesicles than in the smaller cakes.

Modelling of chemical composition

If the evidence from the REE that wholesale incorporation of small quantities of lining into the slag phase has taken place is accepted, then it ought to be possible to estimate the proportion of material involved. A smithing slag might be expected, at a first approximation, to comprise lining material, lost iron, possibly the smith's welding flux plus material from the fuel ash. In reality the situation will be more complex and partial melting of the lining will produce some fractionation; the simplistic approach adopted here can

thus only be considered indicative of the slag-generating reactions.

The approach to mass-balance modelling adopted here is to first estimate the proportion of lining involved by using alumina as the control, and then to calculate the additional iron involved using FeO as control. The difference between the model and the actual slag composition reveals shortfalls in those elements (Ca, Mg, K, P) rich in fuel ash. The calculations are presented in Table 7, with the summary of results in Table 3. An alternative approach by looking at the average dilution of the REE, using the normalisation against lining LYCF04-7, was also attempted, with the results shown in Table 7 in the column labelled REE estimate. In general the results are comparable to those produced from consideration of alumina.

	FeO	lining	SiO ₂	ash
LYC04-1	77.0	15.7	5.1	2.2
LYC04-2	78.0	20.7	0.8	0.5
LYC04-3	82.7	11.5	4.4	1.4
LYC04-4	82.5	10.7	5.7	1.1
LYC04-5A	86.9	12.1	0.0	1.0
LYC04-5B	82.3	16.3	0.0	1.3
LYC04-6	85.0	11.6	1.9	1.5

Table 3. Summary of mass balance modelling of SHC composition. All values in wt%.

All the slags show a high level of loss of oxidised iron from the workpiece, comprising 77-85% of the slag by weight. Lining contributions vary from 11 to 21%, with 0.5 to 2.2% of the slag derived from the fuel ash.

For three samples (LYCF04-1, 3 & 4) there is a significant shortfall in the model for silica, and for two others (LYCF04-2 & 6) there is a lesser shortfall. The silica content of the slags may possibly have been augmented through incorporation of silica from an intentionally added welding flux; on the present evidence however, an origin either through fractionation of the lining or through the lining analysed being less silica-rich than typical are also possible.

Interpretation

Slags produced during iron-working have not received as much research attention as those produced during iron smelting. The recognition of SHCs (also known as plano-convex bases, PCBs) as the major residue from smithing is well established. They have not, in general, been subjected to detailed analysis and the links between slag chemistry and hearth morphology have not yet been investigated. The interpretation of the Coldfurrow assemblage is hampered by a lack of well-described comparative assemblages.

The assemblage is atypical of Romano-British iron working assemblages on two grounds: composition and SHC size.

The material from Coldfurrow lies towards the limit of recorded smithing slag compositions in Britain, in being extremely iron-rich. Comparable compositions are observed however where tuyères were employed (for instance in early medieval Ireland) and the contribution of the hearth ceramics to the slag is reduced. None of the hearth "lining" fragments recovered from this site is certainly from a tuyère, but their use here cannot be excluded.

The mass balance modelling of the slags, although extremely tentative, does give an indication of the extremely low input of hearth lining to the process. Such low contributions suggest that there was little impingement of the hot-zone of the hearth onto the ceramics of the hearth construction. There are usually two such sources in a typical hearth – the zone above the blowhole (either above a simple blowhole, or the upper part of the face of a tuyère) where temperatures are high and melting of the ceramic will add to slag formation from above, and secondly the zone of contact of the iron-rich slag below the blowhole with the adjacent hearth wall. Use of a tuyère reduces the influence of both of these zones by reducing the area of ceramic exposed to the hot-zone above the blowhole and by making any contact between slag and tuyère face occupy only a very small area. Some loss of contact between the slag and wall may also be achieved by the use of high blowing rates, which tends to move the hot-zone away from the point of origin of the air blast. Whatever the precise hearth configuration at Coldfurrow, it is clear that hearth usage did not follow the "typical" Romano-British pattern of the air blast being supplied through a simple blowhole in a clay hearth wall.

The assemblage of SHCs is small (14 complete specimens) and has a mean cake weight of 564g and a maximum of 2077g. These figures indicate that the SHCs produced during smithing at Coldfurrow were significantly larger than those of the measured assemblages at Carmarthen (Crew 2003), Cowbridge (Barford 1996) and Marsh Leys Farm (Young 2005), which are interpreted as blacksmithing residues. Perhaps more relevant are Romano-British assemblages which are likely to include SHCs produced during bloomsmithing. Examples of such assemblages include that from Frocester Court (Price 2000) where a range of smithing hearth cakes/furnace bottoms range up to 2.8kg in weight and accompany iron smelting slags in 2nd-3rd century AD contexts, and also the assemblage from a probably 4th century AD smelting site at Miskin (Young & Macdonald 1998), where complete SHCs certainly range up to 2.2kg. Unfortunately full statistics are unavailable for either site.

Early medieval assemblages from Coolamurry and Carrigoran in Ireland (Young 2006a, b), where some bloomsmithing may have been undertaken, also show a rather similar size distribution to the Coldfurrow assemblage. The Coldfurrow statistics also bear comparison with medieval assemblages from Worcester and Burton Dasset (McDonnell 1991, 1992; McDonnell & Swiss 2004) which are assumed to be from blacksmithing, but which have a much younger age.

Discussion

The interpretation of the Coldfurrow assemblage remains somewhat problematic. The significance of the unusual chemical composition of the smithing slags is uncertain given the present dearth of comparative analyses. Although tuyères are widely known from non-ferrous metalworking contexts on Romano-British sites, they have not been widely recorded from iron working contexts.

Equally, a lack of comparative data makes interpretation of the relatively large size of the SHCs in the Coldfurrow difficult to interpret. The size distribution would suggest that bloomsmithing might have been undertaken on the site. The site has produced no

evidence for iron smelting, but this is not necessarily a reason to indicate bloomsmithing would be unlikely; commonly the two stages of the production of bloomery iron were separated, with smelting commonly being undertaken in rural settings close to the charcoal supplies and bloomsmithing taking place in settlements. Lyonshall is not in an area of known iron ore occurrence, but lies at about 40km from the northern edge of the Forest of Dean, which places it just within the zone of influence of Dean, within which iron ore was transported out from the mining districts to be smelted using local fuel supplies.

An alternative interpretation to the slags representing (at least partially) the residues from bloomsmithing would be the possibility that the production of large slag cakes during smithing was the product of the way the hearths were used. Large slag cakes of iron-rich slag were produced during blacksmithing in early christian and later Ireland in hearths blown using large tubular tuyères. There has not yet been any indication of this tradition of iron working in Roman Britain, but somewhat similar tuyères have recently been recovered from a late Iron Age site in Cornwall (Young 2006c) and the possibility cannot be ruled out at present.

The feature tentatively associated with smithing during excavation (C1561) is unusual deep (0.80m) for a smithing hearth. The nature of this feature remains uncertain.

References

- BARFORD, P.M. 1996. The metalworking debris from Bear Barn and the Bear Field. Pp. 205-209 in: J. Parkhouse & E. Evans, *Excavations in Cowbridge, South Glamorgan, 1977-88*. BAR, British Series 245.
- CREW, P. 2003. Slags and other iron-working residues. pp. 333-340 in: H. James, *Roman Carmarthen: Excavations 1978-1993*. Britannia Monograph Series 20, Society for the Promotion of Roman Studies 2003.
- McDONNELL, G & SWISS, A. 2004. Ironworking residues, pp. 368-378 in: H. Dalwood & R. Edwards, *Excavations at Deansway, Worcester, 1988-89, Romano-British small town to late medieval city*. CBA Research Report 139.
- McDONNELL, G. 1991. A model for the formation of smithing slags, *Materialy Archaeologiczne*, **26**, 23-7.
- McDONNELL, G. 1992. *The identification and analysis of the slags from Burton Dasset, Warwickshire*, English Heritage Ancient Monuments Laboratory report 46/92.
- PRICE, E.G. 2000. *Frocester, A Romano-British Settlement, its antecedents and successors. Volume 2: the Finds*, Gloucester and District Archaeological Research Group.
- TAYLOR, S.R. & McLENNAN, S.M. 1981. The composition and evolution of the continental crust: rare earth element evidence from sedimentary rocks. *Philosophical Transactions of the Royal Society*, **A301**, 381-399.
- YOUNG, T.P. 2004. Evaluation of metallurgical residues from Coldfurrow, Lyonshall (LYCF04). *GeoArch Report 2004/08*. 2pp.
- YOUNG, T.P. 2005. Evaluation of metallurgical residues from Marsh Leys Farm. *GeoArch Report 2005/07*. 10pp.
- YOUNG, T.P. 2006a. Evaluation of archaeometallurgical residues from N30 Moneytucker – Jamestown, sites 1, 4, 5 and 7 (04E0329, 04E0326, 04E0325, 04E0323). *GeoArch Report 2005/13*. 20pp.
- YOUNG, T.P. 2006b. Evaluation of archaeometallurgical residues from Carrigoran, Co. Clare (98E0338). *GeoArch Report 2005/18*. 12pp.
- YOUNG, T.P. 2006c. Evaluation of archaeometallurgical residues from the Richard Lander School, Truro (RLS 04). *GeoArch Report 2006/06*. 15pp.
- YOUNG, T.P. & MACDONALD, P. 1998. Miskin, School Road. *Archaeology in Wales*, **37**, 79.

Plate Captions

Plate 1.

LYCF04-2

(a) Texture in a vesicle-fill towards top of the specimen. Coarse equant fayalite (mid grey) following sparse early wustite (white). Interstitial space largely occupied by leucite-wustite syntectic. Scale bar 300µm.

(b) Heterogeneous texture in upper part of specimen. Early wustite (white) between former vesicles now filled with elongate olivine. Surviving porosity black. Scale bar 1mm.

(c) Wustite dominated texture in main body of cake. Early dendritic wustite (white) followed by elongate olivine (mid grey). Scale bar 800µm.

(d) Detail of infilled vesicle in upper centre of (b). The heterogeneous texture of wustite- and olivine-dominated areas (early vesicles?) bears a late vesicle with an infill dominated by olivine (mid grey) and which has a leucite (dark grey) rim. Surviving porosity, lower right, has a lining of secondary oxides. Scale bar 400µm.

LYCF04-3

(e) Heterogeneous distribution of wustite (light grey), with former vesicles filled by olivine and secondary corrosion products (upper left). Surviving porosity black. Scale bar 2mm.

(f) Detail from central part of (a). Extant porosity (black; lower right) is lined by secondary minerals on top of the original rim of leucite-wustite. The early wustite (lower left) has an interstitial phase of an olivine-leucite syntectic. The vesicle in the upper left is filled with secondary corrosion products. Scale bar 300µm.

LYCF04-4

(g) Texture from the upper part of the specimen showing early wustite dendrites (white) followed by elongate olivine (pale grey) with interstitial glass (mid grey) bearing fine olivine dendrites. Scale bar 80µm.

(h) Texture broadly similar to that of (g), but the interstitial material is in this case largely a leucite-wustite syntectic (dark grey and white). Scale bar 100µm.

(i) Complicated textures close to a large vesicle (out of field of view to left). Shows early wustite (white) followed by olivine (pale grey). The olivine is locally followed by an intergrowth of olivine and a leucite-wustite syntectic. Interstitial glass with fine olivine dendrites also bears a relict quartz grain (left of middle bottom). Two small vesicles on left are filled with secondary corrosion products. Scale bar 300µm.

(j) Margin of a surviving vesicle (black) with large associated growths of a leucite-wustite syntectic. Early wustite dendrites are rather sparse and the olivine is blocky. Scale bar 400µm.

(k) Transect across specimen. Base is just out of view to bottom. This wide view shows the patchy development of wustite across the specimen, with late vesicle fills showing progressively less wustite. Scale bar 2mm

Plate 2.

LYCF04-5a

(a) Typical coarse-grained wustite of lower part of the specimen. Scale bar 800µm.

(b) Vesicle in lower part of wustite-dominated material, infilled with minor wustite, olivine and interstitial leucite-wustite syntectic. Scale bar 1mm.

(c) Detail from central part of the vesicle fill in (b). Olivine pale grey, wustite white, leucite dark grey. Scale bar 200µm.

LYCF04-5b

(d) Detail of texture in upper part of the specimen, with early wustite (white) followed by olivine (pale grey), with interstitial glass bearing fine olivine dendrites. Scale bar 100µm.

(e) Texture of upper part of specimen. Detail in (a) is drawn from left centre. Coarse wustite (white) is followed by large elongate olivine (pale grey) with crystals of up to 800x200µm. Scale bar 800µm.

(f) Detail showing marked contact in the lower part of the specimen between coarse wustite as seen in LYCF04-5a and the overlying olivine with interstitial leucite-wustite syntectic. The similarity of this to the vesicle-fill material lower in the cake (e.g. (c)) suggests that this is the margin of an extremely large vesicle, rather than layering. Scale bar 300µm.

Catalogue

1103 564g. Small irregular plano-convex smithing hearth cake, tapering to one end. Base probably a charcoal contact with descending prills at proximal end and top probably smooth, but both obscured by rust. Internal corrosion is starting to cause the piece to explode. Very dense and presumably contains some metallic iron. 115x100x50mm

1106 Small fragment of lining (16g) as 1511/1517.

1511 c. 40 pieces of smithing debris. Three pieces are substantially complete SHCs:

The largest is 100x120 wide x 40mm deep plano-convex cake. This SHC weighs 450g, has a rough to microprilly base and a top with raised slag lobes; sampled as LYCF04-2.

176g, a slab-like SHC with a slightly crescentic shape with possible poker hole in centre of the concave face. Lower face rusty with smooth charcoal impressions over most of surface, but has clay adhering to one end. Top smooth blown, dense.

182g, very deformed but possibly complete slab-like cake. Top smooth blown, base with small charcoal dimples.

Several pieces of hearth lining are extremely sandy and fired pink. 1603g total

1517 slab (102g) of well flowed (and relined?) hearth wall. Vitrified surface convex. Rear of specimen pink (as 1511). Irregular fragment (43g) of rusty vesicular slag with included wall material.

1523 Small fragment, 216g, is an irregular fragment from a large SHC.

Intermediate piece is an irregular, possibly double-layer, SHC weighing 750g, 110x100x50mm. Base prilly, top blown proximally. Sampled as LYCF04-4. Largest piece 1015g, 160x110x60mm, is substantial part of SHC with mixed sintered/microdimpled base, major cut mark on one end - apparently from quite a broad tool about 50mm wide, very dense, wide, flat cake. Probably 90% of original SHC.

1526 3 very granular hearth cakes. Largest piece is a 765g SHC sampled as LYCF04-3, which has a vesicular bowl with a slightly more charcoal-rich fill and a raised dense central area to the upper surface. Intermediate piece is part or all of a thin SHC of which part of the crust has been flipped onto the top of the remainder, 390g. Smallest piece is part or all of an extremely irregular, probably double-layer SHC weighing 266g

1526 c. 6 pieces (47g) of vitrified lining as 1573/1561

1531 Large plano-convex hearth cake, 2077g, in two pieces (1960 and 117g), 190x150x70mm, sampled as LYCF04-5. Highly vesicular texture with charcoal moulds. 394g piece comprising most (?) of a double layer cake of which the lower layer has strong lobes and appears to have been more fluid. A small piece, 94g comprises a poorly developed wall contact (burr) with some flowage down the wall.

1531 165g fragment of vesicular plano-convex cake.

1540 Not slag. 1 piece of pottery, 3 pieces of reduced fired clay and 1 piece of coal.

1561 1110g of larger pieces, 174g of smaller pieces bagged separately. Assemblage contains a few

pieces of Mn-stained sandstone, but otherwise comprises smithing debris. Concreted material attached to the slag is rich in charcoal and flake hammerscale. No plano-convex pieces, rather the slags are thin and platy, with a granular texture. Two examples are essentially complete (?). One (290g) appears to have had its thin crust folded over on extraction, and is very rough in texture, the second (260g) forms a small rusty, porous SHC, sampled as LYCF04-6.

1561 29g total comprising 9 pieces of slagged lining. Fabric is a red silty clay.

1561 c. 25 pieces of small slag debris, including granular materials. 1 piece of sandstone. 1 piece of fired lining.

1573 Small rusty hearth cake (210g, 115x75x50mm) with very rusty base and better-flowed protrusion, sampled as LYCF04-1, together with a similar fragment (27g). All similar to material from 1561.

1573 c. 16 pieces of variably slagged lining as 1561. Total 307g.

4010 small fragment of coked coal

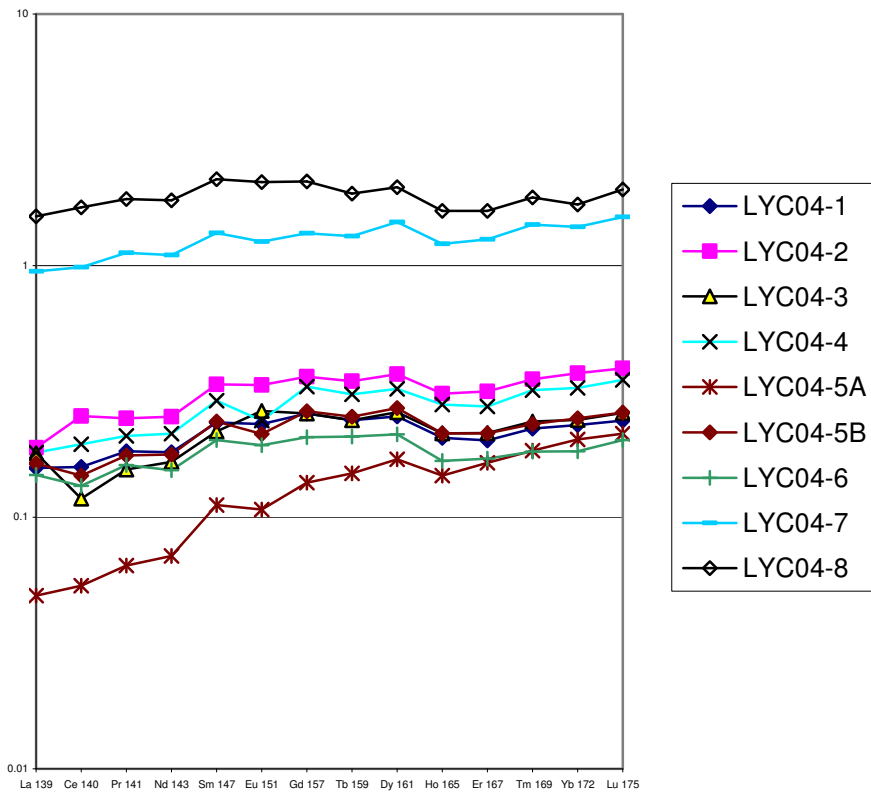


Figure 1. REE profiles normalised against Upper Crust (normalisation factors after Taylor and McLennan 1981)

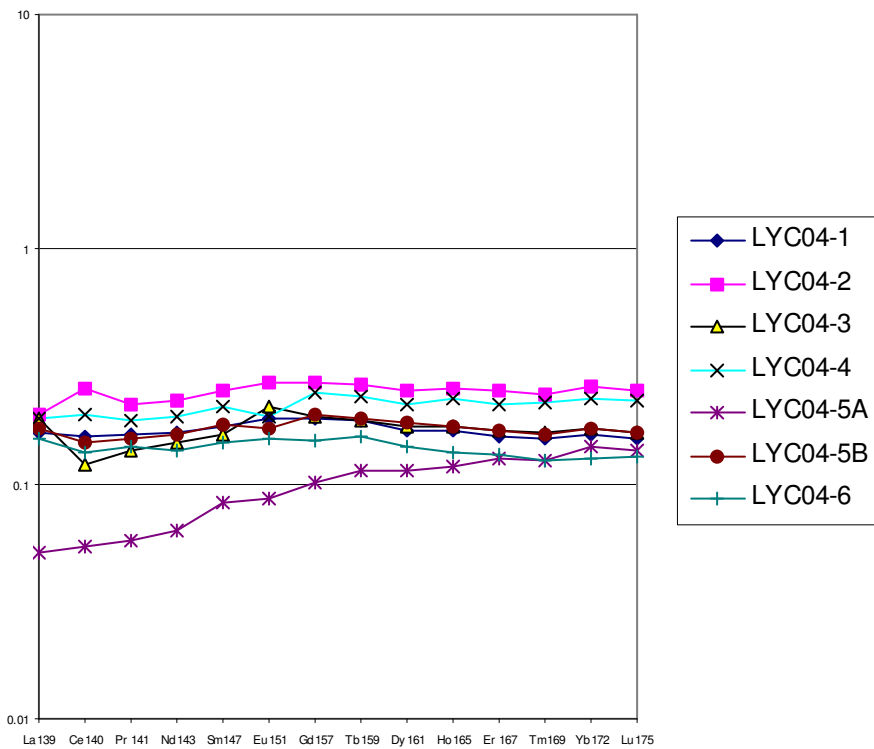


Figure 2. REE profiles for the slags, normalised against lining sample LYCF04-7

Sample	Additional data	SiO ₂	Al ₂ O ₃	Fe ₂ O ₃	FeO	MnO	MgO	CaO	Na ₂ O	K ₂ O	TiO ₂	P ₂ O ₅	LOI	LOI	total
SHCs															
LYC04-1	c1573, 210g	15.42	2.13	81.67	73.49	0.08	0.48	1.56	0.16	0.52	0.13	0.24	-1.92	6.26	100.46
LYC04-2	c1511, 450g	14.38	2.74	80.77	72.68	0.09	0.48	0.45	0.10	0.24	0.19	0.20	1.24	9.33	100.89
LYC04-3	c1526, 765g	11.91	1.56	87.51	78.74	0.11	0.60	0.60	0.10	0.34	0.10	0.32	-2.28	6.49	100.88
LYC04-4	c1523, 750g	13.17	1.51	90.91	81.80	0.08	0.39	0.53	0.16	0.42	0.08	0.24	-6.89	2.22	100.61
LYC04-5A	c1531, 1960g	8.12	1.64	91.22	82.08	0.11	0.43	0.39	0.07	0.40	0.10	0.26	-3.60	5.54	99.13
LYC04-5B	ditto	11.04	2.26	89.08	80.16	0.10	0.52	0.70	0.10	0.53	0.11	0.29	-4.75	4.17	99.99
LYC04-6	c1561, 260g	9.64	1.57	89.78	80.79	0.06	0.44	1.00	0.10	0.37	0.10	0.18	-2.91	6.09	100.33
Lining															
LYC04-7		71.55	14.37	5.06	4.55	0.11	1.99	0.27	0.87	2.06	0.87	0.44	2.31	2.82	99.90
LYC04-8		66.28	16.62	5.45	4.90	0.16	2.57	0.86	0.75	2.10	0.81	1.71	3.04	3.59	100.34

Table 4. Major element analytical data determined by XRF. Fe calculated as Fe₂O₃ and alternatively (shaded in grey) as FeO. LOI = loss on ignition, where shaded in grey recalculated for iron expressed as FeO. All data in wt%.

	Be	V	Cr	Co	Ni	Zn	Ga	Rb	Sr	Y	Zr	Nb	Mo	Sn	Cs	Ba
LYC04-1	0.77	10.5	9.7	7.6	47.8	160.5	5.4	7.3	31.0	5.9	107.9	1.81	2.00	0.56	2.04	184.7
LYC04-2	1.77	30.1	22.1	12.0	45.3	64.4	4.1	3.2	18.0	9.4	76.8	2.57	0.83	0.67	2.09	245.4
LYC04-3	1.86	18.7	9.6	2.7	19.1	24.8	3.2	5.5	22.1	7.0	104.3	1.60	0.71	0.36	2.11	137.0
LYC04-4	1.90	19.7	7.3	3.3	5.1	15.0	3.1	14.2	43.5	9.0	103.5	1.65	0.45	0.39	2.76	141.7
LYC04-5A	1.27	5.8	1.4	5.8	30.9	14.4	4.5	5.2	12.4	4.7	89.5	1.06	0.74	0.05	2.80	124.4
LYC04-5B	1.54	13.8	11.2	3.0	8.2	38.3	3.5	11.5	30.5	6.4	107.0	1.75	0.60	0.49	2.47	206.8
LYC04-6	0.80	3.1	18.9	1.7	17.8	26.8	6.4	9.9	36.8	5.1	109.9	1.72	0.92	0.71	2.59	189.6
LYC04-7	1.35	66.5	100.6	12.0	54.7	146.1	18.1	68.6	49.6	32.1	313.5	10.53	1.31	1.44	6.32	209.7
LYC04-8	1.34	45.3	47.6	14.0	33.1	205.2	21.6	94.5	53.5	42.7	374.2	10.70	1.51	1.48	7.11	164.6

Table 5a. Minor and trace elements determined by ICP-MS. All data in ppm.

	La	Ce	Pr	Nd	Sm	Eu	Gd	Tb	Dy	Ho	Er	Tm	Yb	Lu	Hf	Ta	Th	U	Σ REE	U/Th
LYC04-1	4.71	10.12	1.30	4.70	1.07	0.21	0.98	0.16	0.88	0.17	0.46	0.07	0.51	0.08	1.12	0.12	1.68	0.84	25.57	0.50
LYC04-2	5.66	16.12	1.75	6.52	1.51	0.29	1.37	0.22	1.30	0.25	0.73	0.12	0.82	0.12	0.27	0.15	1.94	1.97	36.97	1.01
LYC04-3	5.39	7.58	1.10	4.32	0.99	0.23	0.98	0.16	0.91	0.17	0.50	0.08	0.54	0.08	0.91	0.09	1.25	1.93	23.22	1.54
LYC04-4	5.42	12.46	1.49	5.59	1.31	0.21	1.26	0.20	1.13	0.22	0.63	0.11	0.72	0.11	0.96	0.11	1.45	2.03	32.06	1.40
LYC04-5A	1.46	3.41	0.46	1.82	0.50	0.09	0.52	0.10	0.59	0.12	0.38	0.06	0.45	0.07	0.72	0.08	1.01	1.75	10.18	1.74
LYC04-5B	4.90	9.37	1.25	4.62	1.08	0.19	1.00	0.16	0.95	0.17	0.50	0.08	0.54	0.08	1.11	0.11	1.54	2.09	25.08	1.36
LYC04-6	4.41	8.52	1.14	3.99	0.91	0.17	0.79	0.13	0.75	0.13	0.39	0.06	0.40	0.06	1.11	0.11	1.43	0.92	22.04	0.64
LYC04-7	28.47	63.02	7.98	28.68	6.07	1.10	5.11	0.84	5.22	0.98	2.92	0.48	3.14	0.50	6.69	1.05	12.20	2.17	154.68	0.18
LYC04-8	47.16	108.97	13.05	47.26	9.92	1.89	8.21	1.24	7.18	1.32	3.79	0.62	3.85	0.64	8.32	1.31	15.58	1.77	255.24	0.11

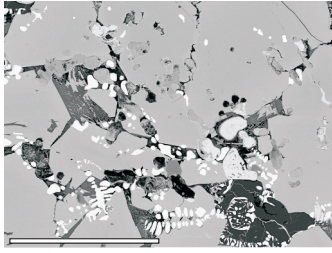
Table 5b. Minor and trace elements determined by ICP-MS. All data in ppm. Σ REE = total concentration of rare earth elements.

	SiO ₂ /Al ₂ O ₃	Σ REE	U/Th	Fe (wt%)	Σ REE/Al (x10 ⁵)
LYC04-1	7.23	25.42	0.50	57.12	22.5
LYC04-2	5.25	36.80	1.01	56.49	25.42
LYC04-3	7.64	23.02	1.54	61.21	27.95
LYC04-4	8.74	30.85	1.40	63.59	38.7
LYC04-5A	4.96	10.03	1.74	63.80	11.6
LYC04-5B	4.88	24.89	1.36	62.31	20.8
LYC04-6	6.13	21.88	0.64	62.80	26.3
LYC04-7	4.98	154.51	0.18	3.54	20.3
LYC04-8	3.99	255.10	0.11	3.81	29.0

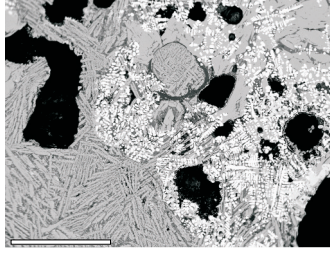
Table 6. Calculated ratios and elemental iron content.

Sample	SiO2	Al2O3	FeO	MnO	MgO	CaO	Na2O	K2O	TiO2	P2O5	LOI	total				
Analyses																
<i>SHC slag</i>																
LYC04-1	15.42	2.13	73.49	0.08	0.48	1.56	0.16	0.52	0.13	0.24	6.26	100.46				
LYC04-2	14.38	2.74	72.68	0.09	0.48	0.45	0.10	0.24	0.19	0.20	9.33	100.89				
LYC04-3	11.91	1.56	78.74	0.11	0.60	0.60	0.10	0.34	0.10	0.32	6.49	100.88				
LYC04-4	13.17	1.51	81.80	0.08	0.39	0.53	0.16	0.42	0.08	0.24	2.22	100.61				
LYC04-5A	8.12	1.64	82.08	0.11	0.43	0.39	0.07	0.40	0.10	0.26	5.54	99.13				
LYC04-5B	11.04	2.26	80.16	0.10	0.52	0.70	0.10	0.53	0.11	0.29	4.17	99.99				
LYC04-6	9.64	1.57	80.79	0.06	0.44	1.00	0.10	0.37	0.10	0.18	6.09	100.33				
<i>Hearth lining</i>																
LYC04-7	71.55	14.37	4.55	0.11	1.99	0.27	0.87	2.06	0.87	0.44	2.82	99.90				
Model													Mix			
													% FeO	% lining additions	REE estimate	
LYC04-1	10.62	2.13	73.49	0.02	0.30	0.04	0.13	0.31	0.13	0.07	0.42	87.23	73%	15%	12%	11%
LYC04-2	13.67	2.74	72.68	0.02	0.38	0.05	0.17	0.39	0.17	0.08	0.54	90.35	72%	19%	9%	17%
LYC04-3	7.76	1.56	78.74	0.01	0.22	0.03	0.09	0.22	0.09	0.05	0.31	88.78	78%	11%	11%	12%
LYC04-4	7.51	1.51	81.81	0.01	0.21	0.03	0.09	0.22	0.09	0.05	0.30	91.52	81%	11%	8%	15%
LYC04-5A	8.13	1.63	82.08	0.01	0.23	0.03	0.10	0.23	0.10	0.05	0.32	92.59	82%	11%	7%	7%
LYC04-5B	11.27	2.26	80.16	0.02	0.31	0.04	0.14	0.32	0.14	0.07	0.44	94.73	79%	16%	5%	12%
LYC04-6	7.83	1.57	80.79	0.01	0.22	0.03	0.10	0.23	0.10	0.05	0.31	90.92	80%	11%	9%	10%
Model minus Analysis													Additions			
													SiO2	CaO+K2O+MgO+P2O5	volatiles	
LYC04-1	-4.79	0.00	0.00	-0.06	-0.18	-1.52	-0.03	-0.21	0.00	-0.17	-5.84	-12.81	4.79	2.09	5.84	
LYC04-2	-0.72	0.00	0.00	-0.07	-0.10	-0.39	0.06	0.16	-0.02	-0.12	-8.79	-9.99	0.72	0.45	8.79	
LYC04-3	-4.15	0.00	0.00	-0.10	-0.39	-0.57	0.00	-0.12	-0.01	-0.27	-6.18	-11.79	4.15	1.35	6.18	
LYC04-4	-5.66	0.00	0.00	-0.07	-0.19	-0.50	-0.07	-0.21	0.01	-0.19	-1.92	-8.79	5.66	1.09	1.92	
LYC04-5A	0.01	0.00	0.00	-0.10	-0.20	-0.36	0.03	-0.17	0.00	-0.21	-5.22	-6.23		0.94	5.22	
LYC04-5B	0.23	0.00	0.00	-0.08	-0.21	-0.66	0.04	-0.20	0.03	-0.22	-3.73	-4.82		1.29	3.73	
LYC04-6	-1.81	0.00	0.00	-0.05	-0.22	-0.97	0.00	-0.14	0.00	-0.13	-5.78	-9.10	1.81	1.46	5.78	

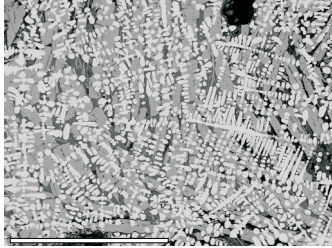
Table 7. Modelling of SHC slag composition in terms of a mixture of hearth lining (calculation based on balancing Al2O3), with added FeO. The model compositions show a shortfall in elements derived from the fuel ash (Ca, K, Mg, P), and, in some cases, in silica. The shortfall in LOI is caused by the high carbon content of the slag specimens because of charcoal inclusions. The figures labelled REE estimate are the estimates for the proportion of lining in the mixture based on the REE content rather than alumina, derived from the average REE dilution observed through normalisation against LYCF04-7.



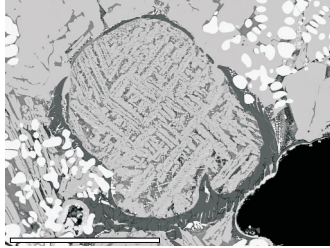
a



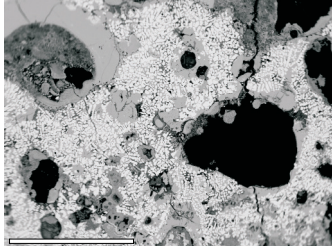
b



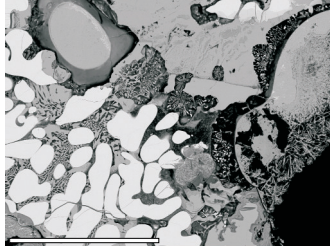
c



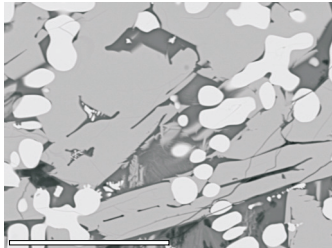
d



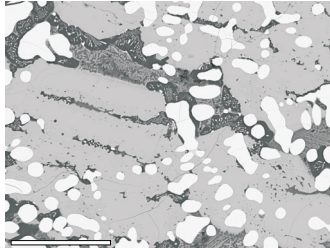
e



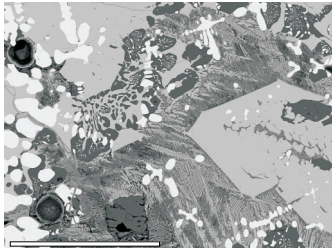
f



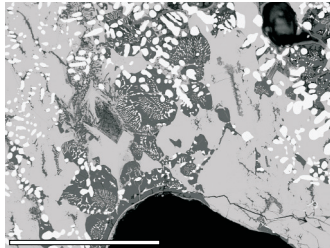
g



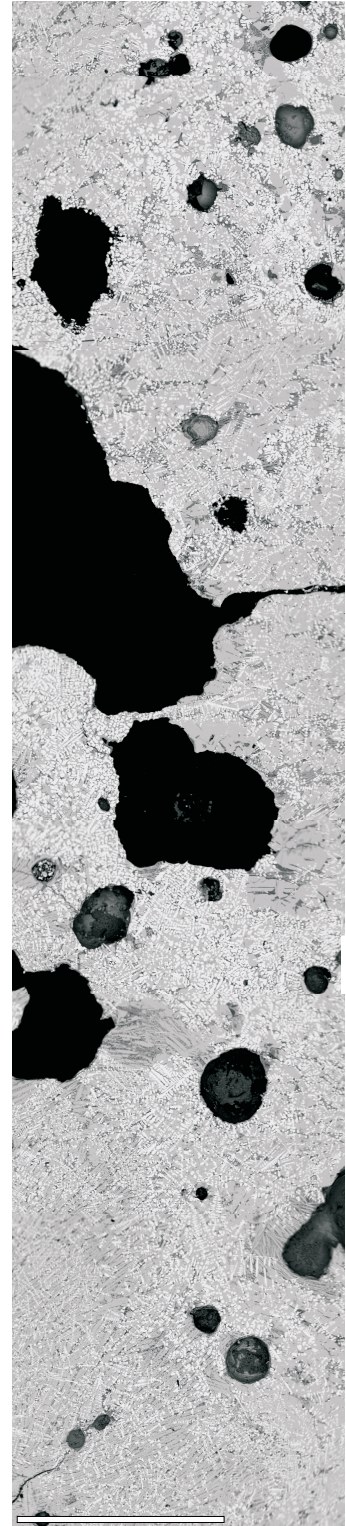
h



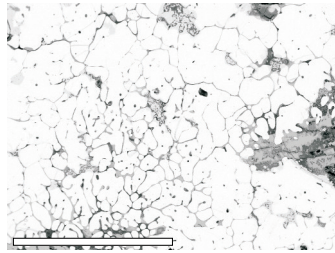
i



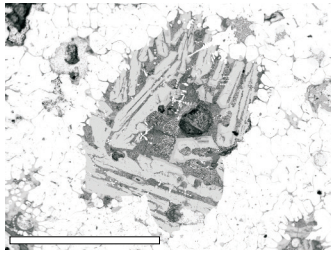
j



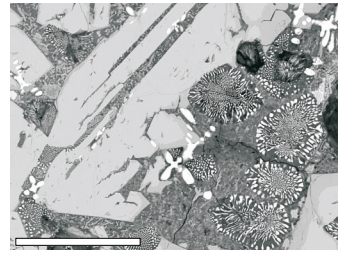
k



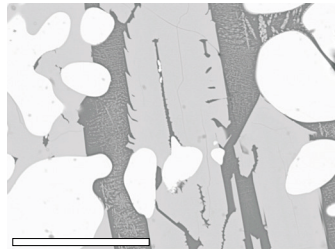
a



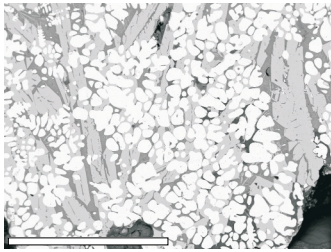
b



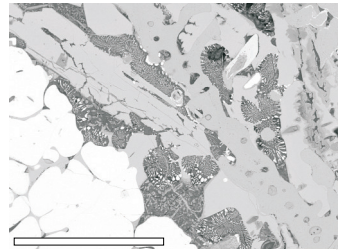
c



d



e



f

Plate 2

GeoArch



geoarchaeological, archaeometallurgical & geophysical investigations

54 Heol y Cadno,
Thornhill,
Cardiff,
CF14 9DY.

Mobile:
Fax:
E-Mail:
Web:

07802 413704
08700 547366
Tim.Young@GeoArch.co.uk
www.GeoArch.co.uk